AIP | Review of Scientific Instruments

A high-flux high-order harmonic source

P. Rudawski, C. M. Heyl, F. Brizuela, J. Schwenke, A. Persson, E. Mansten, R. Rakowski, L. Rading, F. Campi, B. Kim, P. Johnsson, and A. L'Huillier

Citation: Review of Scientific Instruments **84**, 073103 (2013); doi: 10.1063/1.4812266
View online: http://dx.doi.org/10.1063/1.4812266
View Table of Contents: http://scitation.aip.org/content/aip/journal/rsi/84/7?ver=pdfcov
Published by the AIP Publishing

A high-flux high-order harmonic source

P. Rudawski,[1,a)] C. M. Heyl,[1] F. Brizuela,[1] J. Schwenke,[1] A. Persson,[1] E. Mansten,[2] R. Rakowski,[1] L. Rading,[1] F. Campi,[1] B. Kim,[1] P. Johnsson,[1] and A. L'Huillier[1]
[1]*Department of Physics, Lund University, P.O. Box 118, SE-221 00 Lund, Sweden*
[2]*MAX-lab, Lunds Universitet, P.O. Box 118, SE-221 00 Lund, Sweden*

(Received 12 March 2013; accepted 11 June 2013; published online 9 July 2013)

We develop and implement an experimental strategy for the generation of high-energy high-order harmonics (HHG) in gases for studies of nonlinear processes in the soft x-ray region. We generate high-order harmonics by focusing a high energy Ti:Sapphire laser into a gas cell filled with argon or neon. The energy per pulse is optimized by an automated control of the multiple parameters that influence the generation process. This optimization procedure allows us to obtain energies per pulse and harmonic order as high as 200 nJ in argon and 20 nJ in neon, with good spatial properties, using a loose focusing geometry ($f_{\#} \approx 400$) and a 20 mm long medium. We also theoretically examine the macroscopic conditions for absorption-limited conversion efficiency and optimization of the HHG pulse energy for high-energy laser systems. [http://dx.doi.org/10.1063/1.4812266]

I. INTRODUCTION

High-order harmonics generated by the nonlinear interaction of an intense ultrashort laser pulse with atoms or molecules are now used in many fields of physics. The interest in the generated radiation results from unique features like tunability over the extreme ultraviolet (XUV) and soft x-ray (SXR) spectral regions (reaching several keV[1,2]), excellent beam quality,[3] and ultrashort pulse duration down to the attosecond range.[4] High-order harmonic generation (HHG) sources are well established in many research areas such as attosecond science[5] or femtosecond spectroscopy[6] and have become interesting for high-resolution imaging,[7,8] free-electron-laser seeding,[9] and nonlinear optics in the XUV range.[10,11]

Most applications of HHG sources benefit from harmonic pulses with high pulse energy. This requirement is difficult to achieve due to the low conversion efficiency of the generation process. Since the discovery of the HHG process over two decades ago,[12,13] its conversion efficiency has been progressively improved by optimizing the macroscopic phase-matching conditions and the microscopic single atom response. High-order harmonic generation has been carried out in different conditions, such as high-pressure jets,[14] gas cells,[15] semi-infinite media, and capillaries.[16] Phase-matching optimization using loosely focused (possibly self-guided) fundamental fields has led to conversion efficiencies of $\sim 10^{-7}$ in neon,[15] $\sim 10^{-5}$ in argon,[17] and slightly below 10^{-4} in xenon.[18,19] By modifying the generation field, e.g., by combining the fundamental field with one or more of its harmonics, the microscopic single atom response has been controlled on the subcycle level leading to enhanced HHG signals and/or generation of even-order harmonics.[20–22]

In this article, we describe a high-flux HHG source operating in the photon energy range up to 100 eV. The HHG setup is designed to work in a loose focusing geometry (up to 5 m focal length) and is driven by a high energy femtosecond laser system delivering up to 100 mJ per pulse. The optimization of the signal is performed using an automated scan of the main parameters that contribute to phase-matching (e.g., driving pulse intensity, gas pressure, etc.). Using this technique we have obtained a total energy per pulse in argon of a microjoule and a few hundred nJ in neon, in a geometry with an f-number $f_{\#} = f/D \approx 400$ and $f_{\#} \approx 133$, respectively, and a 20 mm long gas cell. Beam profiles were measured using an XUV-camera and the coherence properties were estimated in a Young's double-slit experiment. The article is organized as follows. Section II presents theoretical considerations for HHG under loose focusing. The HHG setup together with the methods for characterization and optimization are described in Sec. III. Results obtained with the high-energy, ultrashort laser system at the Lund Laser Centre are presented in Sec. IV. Section V presents a summary of the work and a discussion about scaling to extremely long focal lengths.

II. MODEL FOR LOOSE FOCUSING HHG

High-order harmonic generation with high conversion efficiency requires optimization of both the microscopic and macroscopic properties of the process. The microscopic response is well described by a semi-classical three-step model.[23,24] In every half-cycle of the driving wave, electrons can tunnel through the distorted atomic potential barrier, being then accelerated in the intense laser field. Depending on the release time into the continuum, the electrons may return to the parent ion and recombine, emitting an XUV photon. The trajectories of these electrons can be divided into two groups called short and long, depending on the excursion time in the continuum. HHG requires laser intensities in the range of 10^{14} W/cm^2–10^{15} W/cm^2 depending on the selected gas.

a)Electronic mail: piotr.rudawski@fysik.lth.se

Macroscopically, the total HHG signal is a coherent sum of the photons emitted from different atoms in the medium. For a given harmonic order q, constructive addition occurs along the propagation direction over the so-called coherence length $L_{\mathrm{coh}} = \pi/\Delta k$. Here, $\Delta k = qk_1 - k_{\mathrm{q}}$ is the wave-vector mismatch along the propagation direction between the generated field and the laser-induced polarization at frequency $q\omega$. In order to maximize the coherence length, the wave-vector mismatch must be minimized. In a non-guiding focus geometry this can be done through the interplay between the four sources of wave-vector mismatch,

$$\Delta k = \underbrace{\Delta k_{\mathrm{g}}}_{<0} + \underbrace{\Delta k_{\mathrm{n}}}_{>0} + \underbrace{\Delta k_{\mathrm{p}}}_{<0} + \underbrace{\Delta k_{\mathrm{d}}}_{\substack{<0 \text{ for } z<0 \\ >0 \text{ for } z>0}}. \quad (1)$$

The negative contribution Δk_{g} originates from the Gaussian beam phase gradient along the propagation direction (z). Δk_{n} and Δk_{p} describe the neutral and free-electron dispersion which have opposite sign and are proportional to the gas pressure. To explicitly outline this linear dependence, we write $\Delta k_{\mathrm{n,\,p}} = p\,\partial(\Delta k_{\mathrm{n,\,p}})/\partial p$, where the partial derivative is now pressure independent in the following. Δk_{d} is the gradient of the so-called dipole phase which is proportional to the intensity gradient and is small for the short trajectories but large for the long ones.[25]

Under our experimental conditions, the short trajectories dominate the HHG process. If only these trajectories are considered in Eq. (1), the dipole phase contribution can be neglected and the wave-vector mismatch can be minimized by canceling the plasma dispersion and Gaussian beam phase gradient with the neutral dispersion. For a fixed generation geometry, the degree of ionization in the medium determines the pressure, p_{match}, for which the system is phase matched.[26,27] For each harmonic order, p_{match} is defined as

$$p_{\mathrm{match}} = -\frac{\Delta k_{\mathrm{g}}}{\frac{\partial(\Delta k_{\mathrm{n}})}{\partial p} + \frac{\partial(\Delta k_{\mathrm{p}})}{\partial p}}. \quad (2)$$

For a given medium, harmonic order, and focal length, the only variable parameter is the free-electron contribution which is proportional to the degree of ionization ($\partial\Delta k_{\mathrm{p}}/\partial p \propto r_{\mathrm{ion}}$), and consequently can be adjusted by changing the laser intensity. The equation requires the intensity to be low enough so that the contribution due to neutral dispersion dominates over the free-electron dispersion. This defines a maximum ionization degree ($r_{\mathrm{ion}}^{\mathrm{max}}$), typically a few percent, above which phase-matched generation is not possible.

Figure 1 shows the variation of p_{match} in argon as a function of the degree of ionization for three harmonic orders and two different focusing geometries. p_{match} tends towards infinity when r_{ion} reaches $r_{\mathrm{ion}}^{\mathrm{max}}$. At low degree of ionization, the phase-matching pressure varies little both with pressure and with harmonic order. Considering that the dipole response is highest at the highest intensity, one could assume that the most efficient generation is possible at high pressures and at intensities that support an ionization degree around $r_{\mathrm{ion}}^{\mathrm{max}}$. High intensities, however, lead to steep gradients of r_{ion} in the longitudinal and radial directions within the generation volume, confining phase-matched generation to a small volume and leading to transient phase-matching.[27] In spite of a higher single atom response at high intensity, those effects can reduce the overall efficiency. An optimum ionization degree should assure phase-matched HHG over a broad bandwidth and a large volume. The ionization level should be such that the phase-matching pressure is approximately constant for a broad range of high-order harmonics, potentially leading to short and intense attosecond pulses. This phase-matching bandwidth increases with decreasing ionization degree yet at the same time the single atom response as well as the conversion efficiency decrease. As a rule of thumb, the optimum value for the ionization degree can be taken as $\sim r_{\mathrm{ion}}^{\mathrm{max}}/2$ for the highest harmonic in the considered HHG bandwidth. Under the conditions of Figure 1, this corresponds to ~2% ionization and a laser intensity of $\sim 1.1 \times 10^{14}$ W/cm^2.

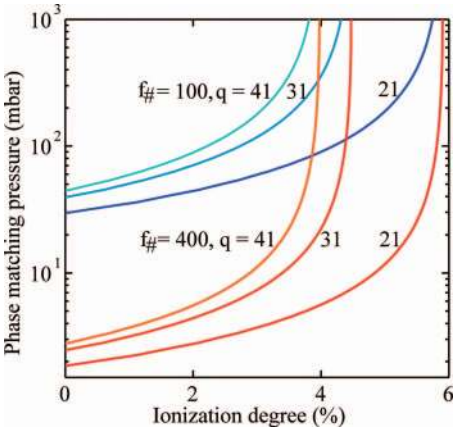

FIG. 1. Phase matching pressure in Ar as a function of ionization degree for different harmonic orders, q, and different focus geometries $f_{\#} = 100$, blue, and $f_{\#} = 400$, red. The central wavelength is 800 nm and the generation cell is placed at the focus of the fundamental beam.

When the coherence length, L_{coh}, is maximized, the harmonic emission is limited by re-absorption in the generation gas. The absorption length, L_{abs}, is defined by

$$L_{\mathrm{abs}}(p) = \frac{kT}{p\sigma_{\mathrm{ion}}}, \quad (3)$$

where k is the Boltzmann constant, T the temperature, and σ_{ion} the ionization cross-section. Following the argumentation of Constant *et al.*,[28] the harmonic yield is then maximized when the medium length, L_{med}, is at least three times the absorption length. This allows to define an optimum medium length under phase-matched conditions, $L_{\mathrm{med}}^{\mathrm{opt}} = 3L_{\mathrm{abs}}(p_{\mathrm{match}})$. For example for the 21st harmonic in Ar, and $f_{\#} = 400$, $T = 300$ K, $\sigma_{\mathrm{ion}} = 2 \times 10^{-21}$ m^2, $p_{\mathrm{match}} \approx 5$ mbar, and consequently $L_{\mathrm{med}}^{\mathrm{opt}}$ should be chosen to be at least 12 mm.

For high-energy laser systems, an increase of the absorption-limited HHG intensity can be achieved by scaling up the $f_{\#}$, i.e., by increasing the focal length for a certain initial beam diameter. The conversion efficiency can be held constant when changing the focal length if the laser pulse energy, the gas pressure, and the medium length are scaled appropriately. Using Gaussian optics and Eqs. (2) and (3), we derive the following scaling relations: E_f (laser energy) $\propto f^2$ in order to keep the same intensity at focus, $p_{\mathrm{match}} \propto 1/f^2$ since $\Delta k_{\mathrm{g}} \propto 1/f^2$, and $L_{\mathrm{med}} \propto f^2$. This ensures constant conversion

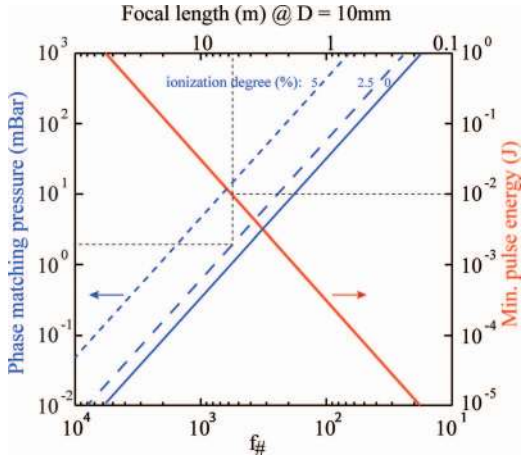

FIG. 2. Scaling of the phase matching pressure and the required laser pulse energy with focal length (or $f_{\#}$) for different ionization levels in argon. The corresponding minimum laser pulse energy required is shown in red. For the simulations, the following parameters were used: beam diameter before focusing: $D = 10$ mm, gas cell position: at the focus, central wavelength of 800 nm, harmonic order $q = 21$. The required pulse energy was calculated assuming a peak intensity of 1.5×10^{14} W/cm^2 and a pulse length of 45 fs.

efficiency, independent of the focusing geometry,[27] and the harmonic energy $E_h \propto f^2$.

Figure 2 illustrates these scaling relations in the case of argon, with the following parameters: 800 nm wavelength, a 45 fs pulse duration, an intensity of 1.5×10^{14} W/cm^2 at focus, and an initial beam diameter of 10 mm. A laser pulse energy of 10 mJ requires a focal length of approximately 5 m and a generation pressure of a few mbar to efficiently generate harmonics.

III. HIGH-ORDER HARMONIC EXPERIMENTAL SETUP

Our HHG setup consists of three sections: generation, diagnostics, and application (see Figure 3). The sections are connected by vacuum tubes with a diameter $\phi = 40$ mm. The generation section is mounted on stiffly connected optical tables. The diagnostics section together with the application chamber are mounted on a rail system. This allows us to adjust the distance between the vacuum chambers depending on the focusing geometry in order to avoid damage of optical elements placed after the generation by the fundamental laser field. It also provides vibration isolation and high stability.

High-order harmonics are generated by loosely focusing a high energy laser beam into a noble gas. The fundamental laser beam is apertured down by a variable diameter iris (I), typically between 9 and 30 mm and focused by a lens (L). Control of the beam size allows for re-adjustments of the focusing geometry ($f_{\#}$) as well as laser energy and intensity distribution at focus. Thus it allows us to optimize phase-matching in a simple way. Directly after the focusing optics, the beam enters the generation chamber. The entrance UV fused silica window is mounted at a small angle to avoid back propagation of the reflected light to the laser system. The beam propagates inside a 100 mm diameter vacuum tube and is folded by mirrors (M) mounted on small breadboards placed in 6-way crosses. Alternatively, the laser beam can be focused by a mirror at near-normal incidence placed in one of the vacuum crosses. The focused beam interacts with the noble gas confined in a cell (PGC). The cylindrical cell has a diameter of typically 0.5 mm and a length between 3 mm and 20 mm. The gas is released at the repetition rate of the laser by a valve[29] driven by a piezo-electric actuator and synchronized with the laser pulse. The opening and closing times are optimized for maximum harmonic signal. Simulating the gas distribution in the cell, we found a small pressure gradient from the middle of the cell, where the gas is injected, towards the ends of the cell, where the pressure abruptly drops. The cell is mounted on an XY motorized stage. Additionally, two motorized actuators control the tilt of the cell with respect to the incoming beam. In order to optimize the position of the cell relative to the laser focus the gas cell is additionally placed on a 6 cm long-range translation stage moving along the propagation direction (Z).

The generation chamber is designed to work simultaneously with up to two gas cells. The cells can be mounted in parallel or in series. The parallel configuration allows for the generation of two independent harmonic beams[30] while the serial configuration can be used for the enhancement of the HHG process using low-order harmonics generated in the first cell.[22] In both configurations, the generated harmonic beam propagates collinearly with the fundamental radiation in vacuum (10^{-6} mbar) to the diagnostics chamber. Elimination

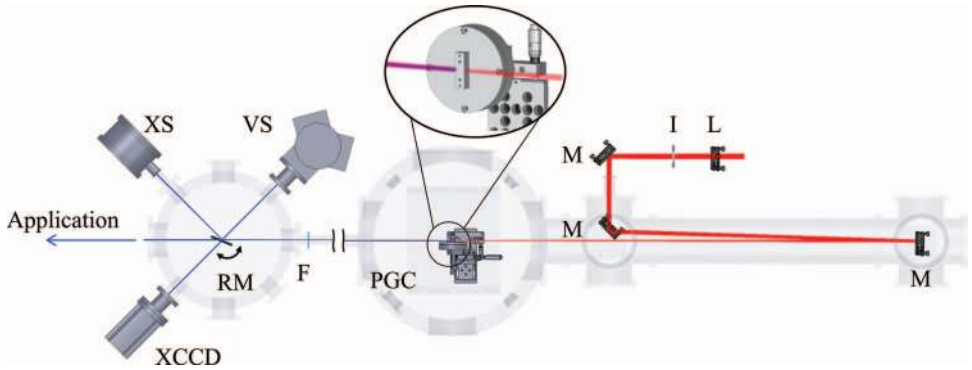

FIG. 3. HHG setup in the 4 m focusing configuration; L - focusing lens, I - iris, M - folding mirrors, PGC - pulsed gas cell, F - aluminum filters, RM - rotating mirror, XS - XUV spectrometer, VS - VUV spectrometer, and XCCD - XUV CCD camera.

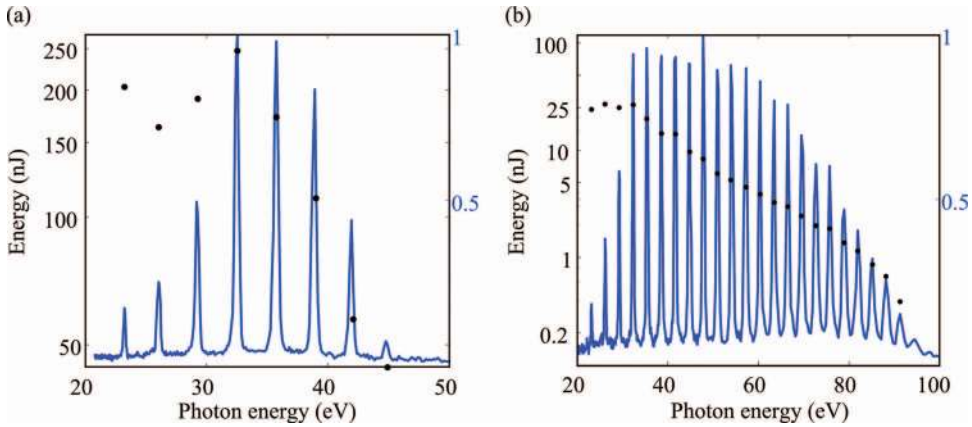

FIG. 4. High-order harmonic spectra in argon (a) and neon (b) gas. The pulse energy per individual harmonics, shown as dots, was obtained by combining total energy measurements with the spectral response from the XUV spectrometer.

of the fundamental is achieved by using 200 nm thick aluminum filters (F). The filters are mounted on a manual translation stage placed at the entrance of the diagnostics chamber, and controlled from the outside of the vacuum chamber.

The alignment of the setup is based on the beam position at the entrance iris and a reference point inside the diagnostics chamber. The precise alignment of the gas cell with respect to the laser beam is done by motorized control of the cell's four axes (XY and two tilts). The reference point and gas cell are monitored by cameras equipped with variable focal length objectives.

At the center of the diagnostics chamber, a gold-coated flat mirror (RM) mounted on a rotation stage is used to send the XUV beam to the different instruments or, when the mirror is removed, towards the application chamber (Fig. 3). The HHG spectra are measured by a flat-field grating spectrometer (XS, Jobin-Yvon PGM-PGS 200). The spectrometer detects spectrally-resolved far-field spatial profiles of individual high-order harmonics in the XUV spectral range. Low-order harmonics are detected using a vacuum ultraviolet monochromator (VS, McPherson 234/302). The vacuum ultraviolet spectrometer is equipped with an MCP detector coated with CsI allowing HHG diagnostics in a range from 50 to 250 nm. Additionally, spatial profiles and energy measurements are carried out using a back-illuminated XUV-CCD (Andor iKon-L) camera (XCCD). To attenuate the HHG beam for these measurements we use one or two 200 nm thick aluminum filters.

IV. RESULTS

This section presents measurements of high-order harmonics generated in argon and neon. The driving laser system is a high-power Ti:Sapphire chirped-pulse-amplification-based laser system delivering 45 fs pulses with up to 100 mJ energy at 10 Hz repetition rate. Before compression, the laser beam is spatially filtered with a conical pinhole mounted in a vacuum chamber. The pinhole waist, approximately 500 μm, is placed in a focal plane of a 1.7 m focal length lens. The laser beam diameter is 30 mm at the entrance to the harmonic setup. The laser beam position and angle are actively stabilized.

Figure 4 presents typical integrated harmonic spectra for (a) argon and (b) neon, recorded by the XUV spectrometer. The driving laser beam, with 20 mJ energy in case of argon and 24 mJ in case of neon, was focused by a 4 m lens in a 20 mm long cell. The HHG cut-off energy is 45 eV (29th harmonic) in argon whereas in neon it reaches 91.5 eV (59th harmonic). Under these conditions the total measured harmonic energy per laser shot is 1.15 μJ for argon and 0.23 μJ for neon. These values correspond to conversion efficiencies of 5×10^{-5} for argon and 8×10^{-6} for neon. Due to the high sensitivity of the XUV camera to the infrared radiation, the harmonic beam energy is measured within the aluminum filter's transmission window, i.e., between 14 eV and 71 eV, corresponding to harmonic orders between 11 and 45. The measurement procedure, similar to the one described by Erny *et al.*,[31] is based on XUV-CCD recorded background-subtracted images. The images are integrated to obtain the total number of counts. The total number of photons is estimated based on a calibration curve from the manufacturer. The individual harmonic energy is obtained by multiplying the total HHG beam energy with the relative intensity of each harmonic measured by the spectrometer. The spectrum is corrected for the folding mirror reflection (based on data from Henke *et al.*[32]), the grating efficiency, and the measured aluminum filter transmission. The estimated pulse energy per harmonic is shown as dots in Figure 4. The most prominent harmonic, both in argon and neon is the 21st harmonic (32.5 eV). Its energy is 250 nJ in argon and 30 nJ in neon. These values are comparable to previous results obtained by Takahashi *et al.*[15,17]

To find the optimum high-order harmonic energies an automated optimization procedure was carried out. This procedure is briefly summarized here. The important parameters to control are: fundamental beam energy and diameter (before focusing), gas pressure, and gas cell position relative to the laser focus. The energy of the fundamental beam is varied by an attenuator consisting of a half-wave plate mounted on a motorized rotation stage and a polarizer. We use a motorized

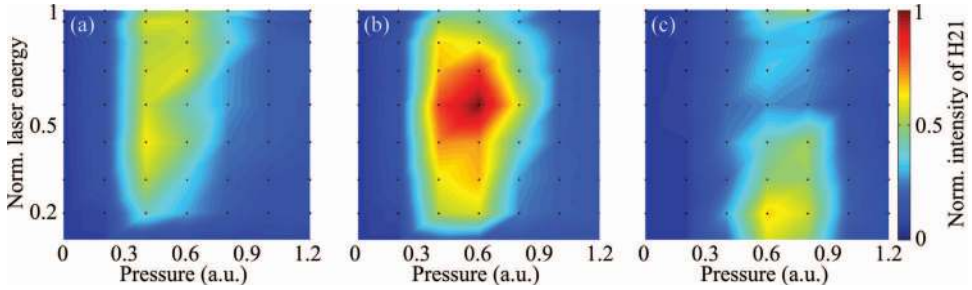

FIG. 5. Intensity of the 21st harmonic generated in argon as a function of driving laser energy and generation gas pressure. The measurements were carried out for a gas cell placed at the laser focus for three iris sizes: (a) $\phi = 22$ mm, (b) $\phi = 24$ mm, and (c) $\phi = 32$ mm. The values of a harmonic intensity between the measured points, shown as black dots, were interpolated.

variable iris to change the diameter of the fundamental beam before focusing. The distance between the center of the cell and the fundamental beam waist is varied by moving the cell. Finally, the gas pressure in the cell is adjusted by controlling a voltage applied to the cell nozzle's piezoelectric disks. We record a set of harmonic spectra while varying these four parameters in an automated way. Either the total HHG energy or the energy of a single harmonic can be optimized. Our optimization procedure allows us to routinely obtain HHG energies at the level of several hundred nJ in argon and a few tens of nJ in neon.

An example of the automated optimization is presented in Figure 5, where we investigated the dependence of the intensity of the 21st harmonic generated in argon as a function of the laser energy and gas pressure for three iris diameters. The signal is normalized to the maximum obtained for 21st harmonic. The recorded data show that for increasing iris size (decreasing $f_{\#}$), the required laser energy decreases and the phase matching pressure increases in agreement with our model prediction (see Fig. 1). Similar optimization in neon shows, as expected, a higher p_{match}. The optimum iris diameter corresponds to the longest Rayleigh range (the highest $f_{\#}$) for which the phase-matching conditions can be achieved, while keeping a high enough intensity at focus. It assures the highest HHG beam energy as is shown in Sec. II.

Figure 6(a) shows the spatial profile of high-order harmonics generated in argon and transmitted through an aluminum filter. The corresponding orders are between 11 and 45. The back-panel shows that the intensity distribution is almost perfectly Gaussian. Similar high quality Gaussian beams were generated in neon. The high spatial quality of the generated beams is due partly to the spatial quality of the driving beam, and partly to optimized phase-matching along the propagation axis. In our conditions, IR and XUV beams distortion due to nonlinear and plasma effects are negligible.

The generated beams divergence carries information about the contribution from the electronic trajectories. The divergence of the "short trajectory" harmonic beam is usually much smaller than for the "long trajectory" harmonics. For the 21st harmonic generated in argon, the divergence of the beam resulting from the long trajectory is 14 times higher than that from the short trajectory.[36] The different divergence is a consequence of a larger accumulated phase on the long trajectories. The analysis of the harmonic beam divergence shows that the main contribution to HHG in our conditions comes from the short trajectories. The contribution from the long trajectories is visible on the analyzed CCD images as a weak background.[30]

To estimate the spatial coherence of the HH beam, we performed a double-slit experiment. The degree of coherence of the HHG beam can be estimated from the fringe contrast in the diffraction pattern.[33,34] The slits used in this experiment had a width of 40 μm, a slit separation of 400 μm, and were located 1.5 m from the source. Figure 6(b) shows a cross-section of the double-slit diffraction pattern obtained with a single shot exposure. The experimental data were fitted with

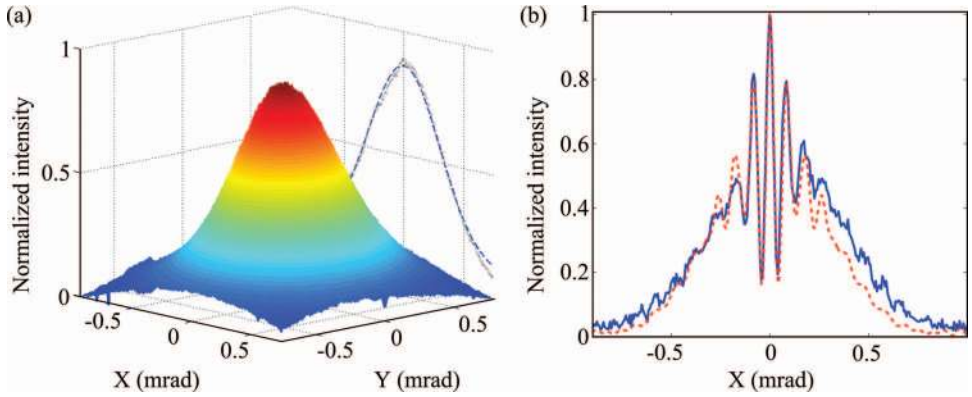

FIG. 6. (a) Spatial profile of the harmonic beam generated in Ar by focusing fundamental radiation with 2 m focal length lens into a 10 mm long cell, recorded with an x-ray CCD camera. The back-panel shows the cross-section of the beam (gray, dotted line), and a fitted intensity distribution (blue, dashed line), (b) Diffraction pattern created in a double-slit experiment, experimental data (blue, solid line), and fitted intensity distribution (red, dashed line).

a theoretical intensity function formed by the sum of diffraction patterns of the different harmonic wavelengths within the transmission window of the filter. The best fit was found with a degree of coherence of 0.8, in good agreement with previous measurements.[35]

V. SUMMARY AND OUTLOOK

We have developed a high-energy HHG setup, working in a loose focusing geometry, generating a total energy per laser pulse of a microjoule in argon and a few hundred nJ in neon. The source is designed for future studies of nonlinear processes in the XUV spectral range. The high harmonic pulse energies together with their high spatial coherence allow us to reach high peak intensities. For example, an intensity of 2×10^{14} W/cm^2 per harmonic pulse could be reached by focusing the HHG beam generated in argon using a broadband grazing-incident mirror, assuming a 3 μm focal spot size, 20 fs duration, and 30% transmission after reflection and filtering by an Al filter.

Our theoretical analysis of phase-matching in the absorption-limited case provides a simple guide for scaling HHG properties to high laser energies. For example we estimate that with $E_f = 1$ J, $f = 50$ m, $p = 0.01$ mbar, and $L_{med} = 6$ m, harmonic pulses with energy as high as 70 μJ could be reached.

Further increase in energy could be achieved by modifying the single atom response, e.g., using a double-cell scheme.[22] Our current beam line includes the option to drive the HHG process with two cells or to use an interferometric setup in order to combine the fundamental with itself, its second or third harmonic (ω/ω, $\omega/2\omega$, and $\omega/3\omega$), thus providing a large range of options for modifying the driving field.

Our experimental results combined with the above considerations show that HHG has the potential to provide intense ultrashort pulses reaching the intensity levels required for nonlinear experiments in the XUV spectral range.

ACKNOWLEDGMENTS

This research was supported by the Marie Curie program ATTOFEL (ITN), the European Research Council (ALMA), the Joint Research Programme ALADIN of Laserlab-Europe II, the Swedish Research Council, the Swedish Foundation for Strategic Research, and the Knut and Alice Wallenberg Foundation.

[1]C. Spielmann, N. H. Burnett, S. Sartania, R. Koppitsch, M. Schnürer, C. Kan, M. Lenzner, P. Wobrauschek, and F. Krausz, "Generation of coherent x-rays in the water window using 5-femtosecond laser pulses" Science **278**, 661 (1997).

[2]T. Popmintchev, M.-C. Chen, D. Popmintchev, P. Arpin, S. Brown, S. Ališauskas, G. Andriukaitis, T. Balciunas, O. D. Mücke, A. Pugzlys, A. Baltuska, B. Shim, S. E. Schrauth, A. Gaeta, C. Hernández-García, L. Plaja, A. Becker, A. Jaron-Becker, M. M. Murnane, and H. C. Kapteyn, "Bright coherent ultrahigh harmonics in the keV x-ray regime from mid-infrared femtosecond lasers," Science **336**, 1287–1291 (2012).

[3]Y. Tamaki, J. Itatani, M. Obara, and K. Midorikawa, "Highly coherent soft x-ray generation by macroscopic phase matching of high-order harmonics," Jpn. J. Appl. Phys. **40**, L1154–L1156 (2001).

[4]E. Goulielmakis, M. Schultze, M. Hofstetter, V. S. Yakovlev, J. Gagnon, M. Uiberacker, A. L. Aquila, E. M. Gullikson, D. T. Attwood, R. Kienberger, F. Krausz, and U. Kleineberg, "Single-cycle nonlinear optics," Science **320**, 1614 (2008).

[5]F. Krausz and M. Ivanov, "Attosecond physics," Rev. Mod. Phys. **81**, 163–234 (2009).

[6]S. L. Sorensen, O. Bjorneholm, I. Hjelte, T. Kihlgren, G. Ohrwall, S. Sundin, S. Svensson, S. Buil, D. Descamps, and A. L'Huillier, "Femtosecond pump-probe photoelectron spectroscopy of predissociative states in acetylen," J. Chem. Phys. **112**, 8038 (2000).

[7]R. L. Sandberg, C. Song, P. W. Wachulak, D. A. Raymondson, A. Paul, B. Amirbekian, E. Lee, A. E. Sakdinawat, C. La-O-Vorakiat, M. C. Marconi, C. S. Menoni, M. M. Murnane, J. J. Rocca, H. C. Kapteyn, and J. Miao, "High numerical aperture tabletop soft x-ray diffraction microscopy with 70-nm resolution," Proc. Natl. Acad. Sci. U.S.A. **105**, 24–27 (2008).

[8]J. Schwenke, E. Lorek, R. Rakowski, X. He, A. Kvennefors, A. Mikkelsen, P. Rudawski, C. M. Heyl, I. Maximov, S.-G. Pettersson, A. Persson, and A. L'Huillier, "Digital in-line holography on amplitude and phase objects prepared with electron beam lithography," J. Microsc. **247**, 196–201 (2012).

[9]G. Lambert, T. Hara, D. Garzella, T. Tanikawa, M. Labat, B. Carre, H. Kitamura, T. Shintake, M. Bougeard, S. Inoue, Y. Tanaka, P. Salieres, H. Merdji, O. Chubar, O. Gobert, K. Tahara, and M.-E. Couprie, "Injection of harmonics generated in gas in a free-electron laser providing intense and coherent extreme-ultraviolet light," Nat. Phys. **4**, 296–300 (2008).

[10]E. P. Benis, D. Charalambidis, T. N. Kitsopoulos, G. D. Tsakiris, and P. Tzallas, "Two-photon double ionization of rare gases by a superposition of harmonics," Phys. Rev. A **74**, 051402(R) (2006).

[11]K. Ishikawa and K. Midorikawa, "Two-photon ionization of He^+ as a nonlinear optical effect in the soft-x-ray region," Phys. Rev. A **65**, 043405 (2002).

[12]M. Ferray, A. L'Huillier, X. F. Li, G. Mainfray, and C. Manus, "Multiple-harmonic conversion of 1064 nm radiation in rare gases," J. Phys. B **21**, L31 (1988).

[13]A. McPherson, G. Gibson, H. Jara, U. Johann, T. S. Luk, I. A. McIntyre, K. Boyer, and C. K. Rhodes, "Studies of multiphoton production of vacuum-ultraviolet radiation in the rare gases," J. Opt. Soc. Am. B **4**, 595 (1987).

[14]T. Brabec and F. Krausz, "Intense few-cycle laser fields: Frontiers of nonlinear optics," Rev. Mod. Phys. **72**, 545 (2000).

[15]E. J. Takahashi, Y. Nabekawa, and K. Midorikawa, "Low-divergence coherent soft x-ray source at 13 nm by high-order harmonics," Appl. Phys. Lett. **84**, 4–6 (2004).

[16]T. Popmintchev, M. C. Chen, P. Arpin, M. M. Murnane, and H. C. Kapteyn, "The attosecond nonlinear optics of bright coherent x-ray generation," Nat. Photonics **4**, 822–832 (2010).

[17]E. Takahashi, Y. Nabekawa, T. Otsuka, M. Obara, and K. Midorikawa, "Generation of highly coherent submicrojoule soft x rays by high-order harmonics," Phys. Rev. A **66**, 021802(R) (2002).

[18]E. Takahashi, Y. Nabekawa, and K. Midorikawa, "Generation of 10-μJ coherent extreme-ultraviolet light by use of high-order harmonics," Opt. Lett. **27**, 1920 (2002).

[19]J.-F. Hergott, M. Kovacev, H. Merdji, C. Hubert, Y. Mairesse, E. Jean, P. Breger, P. Agostini, B. Carré, and P. Salières, "Extreme-ultraviolet high-order harmonic pulses in the microjoule range," Phys. Rev. A **66**, 021801(R) (2002).

[20]J. Mauritsson, P. Johnsson, E. Gustafsson, A. L'Huillier, K. J. Schafer, and M. B. Gaarde, "Attosecond pulse trains generated using two color laser fields," Phys. Rev. Lett. **97**, 013001 (2006).

[21]D. Shafir, H. Soifer, B. D. Bruner, M. Dagan, Y. Mairesse, S. Patchkovskii, M. Yu. Ivanov, O. Smirnova, and N. Dudovich, "Resolving the time when an electron exits a tunneling barrier," Nature (London) **485**, 343–346 (2012).

[22]F. Brizuela, C. M. Heyl, P. Rudawski, D. Kroon, L. Rading, J. M. Dahlström, J. Mauritsson, P. Johnsson, C. L. Arnold, and A. L'Huillier, "Efficient high-order harmonic generation boosted by below-threshold harmonics," Sci. Rep. **3**, 1410 (2013).

[23]P. B. Corkum, "Plasma perspective on strong-field multiphoton ionization," Phys. Rev. Lett. **71**, 1994 (1993).

[24]K. J. Schafer, B. Yang, L. F. DiMauro, and K. C. Kulander, "Above threshold ionization beyond the high harmonic cutoff," Phys. Rev. Lett. **70**, 1599 (1993).

[25]P. Salières, A. L'Huillier, and M. Lewenstein, "Coherence control of high-order harmonics," Phys. Rev. Lett. **74**, 3776 (1995).

[26]S. Kazamias, D. Douillet, F. Weihe, C. Valentin, A. Rousse, S. Sebban, G. Grillon, F. Augé, D. Hulin, and P. Balcou, "Global optimization of high harmonic generation," Phys. Rev. Lett. **90**, 193901 (2003).

[27]C. M. Heyl, J. Güdde, A. L'Huillier, and U. Höfer, "High-order harmonic generation with μJ laser pulses at high repetition rates," J. Phys. B **45**, 074020 (2012).
[28]E. Constant, D. Garzella, P. Breger, E. Mével, C. Dorrer, C. L. Blanc, F. Salin, and P. Agostini, "Optimizing high harmonic generation in absorbing gases: Model and experiment," Phys. Rev. Lett. **82**, 1668 (1999).
[29]Attotech HB.
[30]C. Lyngå, M. B. Gaarde, C. Delfin, M. Bellini, A. L'Huillier, T. W. Hänsch, and C.-G. Wahlström, "Studies of the temporal coherence of high-order harmonics," Phys. Rev. A **60**, 4823 (1999).
[31]C. Erny, E. Mansten, M. Gisselbrecht, J. Schwenke, R. Rakowski, X. He, M. B. Gaarde, S. Werin, and A. L'Huillier, "Metrology of high-order harmonics for free-electron laser seeding," New J. Phys. **13**, 073035 (2011).
[32]B. L. Henke, E. M. Gullikson, and J. C. Davis, "X-ray interactions: Photoabsorption, scattering, transmission, and reflection at $E = 50$-30000 ev, $Z = 1$–92," At. Data Nucl. Data Tables **54**, 181–342 (1993).
[33]M. Born and E. Wolf, *Principles of Optics* (Cambridge University Press, 1999).
[34]B. E. A. Saleh and M. C. Teich, *Fundamentals of Photonics* (John Wiley and Sons, 2007).
[35]R. A. Bartels, A. Paul, H. Green, H. C. Kapteyn, M. M. Murnane, S. Backus, I. P. Christov, Y. Liu, D. Attwood, and C. Jacobsen, "Generation of spatially coherent light at extreme ultraviolet wavelengths," Science **297**, 376 (2002).
[36]X. He, M. Miranda, J. Schwenke, O. Guilbaud, T. Ruchon, C. Heyl, E. Georgadiou, R. Rakowski, A. Persson, M. B. Gaarde, and A. L'Huillier, "Spatial and spectral properties of the high-order harmonic emission in argon for seeding applications," Phys. Rev. A **79**, 063829 (2009).